

**The influence of the cloud shell on tracer budget measurements of
LES cloud entrainment**

JORDAN T DAWE ^{*} AND PHILIP H AUSTIN

Department of Earth and Ocean Sciences, University of British Columbia, Vancouver, BC, Canada.

^{*}*Corresponding author address:* Jordan T Dawe, Department of Earth and Ocean Sciences, University of British Columbia, 6339 Stores Road, Vancouver, BC, V6T 1Z4, Canada.

E-mail: jdawe@eos.ubc.ca

5 Direct measurements of rates of entrainment into and detrainment from cumulus cloud cores
 6 obtained from LES model cloud fields produce values twice as large as those produced from
 7 total water budget calculations. This difference can be explained by three effects: the
 8 presence of a shell of moist air around the cloud cores and drier air at the edge of the cloud
 9 core, the tendency for the mean tracer values of the entrained fluid to be greater than the
 10 mean tracer value of the cloud shell, and numerical errors in the calculation of the tracer
 11 budget. Preferential entrainment of shell air that is moving upward faster than the mean shell
 12 creates strong vertical momentum fluxes into the cumulus cloud core, making the assumption
 13 that cumulus clouds entrain fluid with zero vertical momentum incorrect. Variability in the
 14 properties of the moist cloud shell has strong impacts on entrainment values inferred from
 15 tracer budget calculations. These results indicate the dynamics of the cloud shell should be
 16 included in parametrization of cumulus clouds used in general circulation models.

17 1. Introduction

18 The rate at which air is entrained into and detrained from cumulus clouds affects cloud
 19 properties, cloud top height, and vertical transports of heat and moisture. Proper simula-
 20 tion of cumulus sub-grid scale fluxes in General Circulation Models (GCM) depends on the
 21 accurate parametrization of entrainment of environmental tracer properties into the clouds
 22 and detrainment of cloud properties into the environment (Bechtold et al. 2008; de Rooy
 23 and Siebesma 2010).

Entrainment and Detrainment may be defined mathematically as

$$E = -\frac{1}{A} \oint_{\hat{\mathbf{n}} \cdot (\mathbf{u} - \mathbf{u}_i) < 0} \rho \hat{\mathbf{n}} \cdot (\mathbf{u} - \mathbf{u}_i) dl \quad (1a)$$

$$D = \frac{1}{A} \oint_{\hat{\mathbf{n}} \cdot (\mathbf{u} - \mathbf{u}_i) > 0} \rho \hat{\mathbf{n}} \cdot (\mathbf{u} - \mathbf{u}_i) dl \quad (1b)$$

where E and D are the entrainment and detrainment rates in $\text{kg m}^{-3} \text{s}^{-1}$, ρ is the density of air in $\text{kg m}^{-3} \text{s}^{-1}$, \mathbf{u} is the velocity of the air in m s^{-1} , \mathbf{u}_i is the velocity of the cloud surface in m s^{-1} , A is the area of the cloud in m^2 , $\hat{\mathbf{n}}$ is a unit vector directed out the cloud surface, and the path integral is taken around the cloud surface at a constant vertical level (Siebesma 1998). Entrainment and detrainment are thus caused by differences between the motion of the cloud surface and the motion of the air. This includes not just mixing processes, but also adiabatic processes such as condensation of fluid at cloud base. Many parameterizations use cloud core as the region over which to consider entrainment and detrainment, defined as regions having condensed liquid water, positive buoyancy, and upward vertical velocity. In this case, the motion of the cloud core surface is simply substituted for the motion of the cloud surface in equations (1).

Entrainment and detrainment rates impact GCM parametrizations in several ways. First, profiles of cloud vertical mass flux are usually calculated from parametrized entrainment values using the continuity equation for a simple entraining plume to represent an ensemble of cumulus clouds:

$$\rho \frac{\partial a}{\partial t} + \frac{\partial M_{core}}{\partial z} = E - D. \quad (2)$$

Here a is the fractional cloud core area and M_{core} is vertical cloud core mass flux ($\text{kg m}^{-2} \text{s}^{-1}$).

1 The level where the mass flux profile goes to zero then defines the location of the cloud
2 ensemble top. This mass flux profile is combined with the entrainment rate of environmental
3 air into the cloud and the detrainment rate of cloud air into the environment to generate
4 vertical profiles of cloud water vapor, condensate, and temperature, and these profiles are
5 then used to calculate the moistening of the environment by detrainment of cloud fluid
6 (Tiedtke 1989; Kain and Fritsch 1990). Precipitation rates are also generated from the mass
7 flux and tracer profiles produced from the entrainment and detrainment profiles. The wide
8 range of effects that the entrainment and detrainment have make entrainment rate one of
9 the strongest controls on the climate sensitivity of GCMs (Stainforth et al. 2005; Rougier
10 et al. 2009).

Large Eddy Simulation (LES) is the primary tool used to study cloud entrainment and detrainment rates. LES mass entrainment and detrainment rates are typically obtained using budgets of conserved tracer variables to infer the amount of fluid exchange between the cloud ensemble and the surrounding air. Siebesma and Cuijpers (1995) derive the following equations for entrainment and detrainment of mass from the ensemble of cloud core plumes:

$$E_{\phi S}(\phi_{core} - \phi_{env}) = -M_{core} \frac{\partial \phi_{core}}{\partial z} - \frac{\partial \rho a w' \bar{\phi}'^{core}}{\partial z} - \rho a \frac{\partial \phi_{core}}{\partial t} + a \rho \left(\frac{\partial \bar{\phi}}{\partial t} \right)_{forcing} \quad (3a)$$

and

$$D_{\phi S}(\phi_{core} - \phi_{env}) = -M_{core} \frac{\partial \phi_{env}}{\partial z} + \frac{\partial \rho (1-a) \bar{w}' \bar{\phi}'^{env}}{\partial z} + \rho (1-a) \frac{\partial \phi_{env}}{\partial t} - \rho (1-a) \left(\frac{\partial \bar{\phi}}{\partial t} \right)_{forcing} \quad (3b)$$

11 Where ϕ (with units denoted by $[\phi]$) represents any conserved tracer, such as the total specific
12 humidity q_t (kg water kg^{-1} moist air) or the liquid-water moist static energy h (J kg^{-1}); w

1 is vertical velocity (m s^{-1}); *env* and *core* sub- and super-scripts denote horizontally averaged
 2 values conditionally sampled in the cloud environment and core; *forcing* refers to tracer
 3 sources and sinks, such as radiation or subsidence, not included in the other terms; primed
 4 values represent anomalies relative to the horizontal mean; overbars represent horizontal
 5 averaging; and $E_{\phi S}(z)$ and $D_{\phi S}(z)$ are the total mass entrainment into and detrainment
 6 from the cloud core inferred from the tracer budget, in $\text{kg s}^{-1} \text{ m}^{-3}$. We use the S subscript
 7 to differentiate E and D calculated via the Siebesma tracer budget method from other
 8 measures of mass exchanges, and we shall refer to values calculated by this method as
 9 “Siebesma tracer budget” entrainment and detrainment. For convenience, the various tracer
 10 and entrainment/detrainment rate subscripts used below are summarized in the Appendix.

Alternatively, entrainment and detrainment of mass can be calculated directly from the
 LES velocity and tracer fields. Roms (2010) recently presented a technique to measure
 local (grid scale) mass entrainment $e(x, y, z)$ and detrainment $d(x, y, z)$. Summing these
 point measurements horizontally gives $E_d(z)$ and $D_d(z)$, the total mass entrained into and
 detrained from the cloud core field in $\text{kg s}^{-1} \text{ m}^{-3}$, where the d subscript indicates these
 quantities were calculated directly from the model velocity and tracer fields. His equation
 (2) is:

$$e - d = \frac{\partial}{\partial t}(\mathcal{A}\rho) + \nabla \cdot (\rho \mathbf{u} \mathcal{A}) \quad (4)$$

11 Here \mathcal{A} is the “activity” of the fluid, where \mathcal{A} is one at cloud core points and zero otherwise.
 12 The values of $e - d$ are averaged over the time that a grid cell experiences mass fluxes between
 13 an active and an inactive point, then positive $e - d$ values are considered to be purely e , and
 14 negative values, d . As noted above, we shall refer to entrainment and detrainment values

1 calculated by this method as “direct” E and D and denote them with the subscript d .

2 Romps found that such direct calculation of the entrainment and detrainment mass
3 fluxes produced values roughly twice as large as the Siebesma tracer budget calculations.
4 Romps attributed this difference to the Siebesma tracer budget calculation assumption that
5 fluid exchanged between clouds and environment has the mean properties of the cloud or
6 environment at that level, respectively. Studies of the dense, descending shell of moist air that
7 forms around trade-wind cumulus clouds (Jonas 1990; Rodts et al. 2003; Heus and Jonker
8 2008; Jonker et al. 2008; Heus et al. 2009; Wang and Geerts 2010) suggest that the cloud
9 shell properties are quite different than the core or environment properties, bolstering Romps’
10 hypothesis. Since fluid exchanges between clouds and environment must pass through this
11 shell, it is likely that it plays an important role in entrainment and detrainment dynamics.

12 Below we examine the sources of the discrepancy in entrainment and detrainment values
13 calculated via tracer budgets and directly using (4). We show that the discrepancy is ex-
14 plained by three effects: the presence of the shell of moist air around the cloud cores and drier
15 air at the edge of the cloud core, preferential entrainment of shell air with higher average
16 humidity and upward velocity than the mean shell properties which enhances tracer fluxes
17 between the clouds and the environment, and errors in the calculation of the tracer bud-
18 get. We derive a relation to transform the “direct” entrainment flux values into “Siebesma
19 tracer budget” values suitable for use in one-dimensional simple entraining plume cloud
20 parametrizations, and then use these transformed fluxes to evaluate the impact of the shell
21 on tracer budget entrainment and detrainment rates of specific humidity and vertical veloc-
22 ity. Finally, we examine the dynamics that drives the preferential entrainment of air with

1 higher than average specific humidity and vertical velocity.

2 2. Model description

3 All LES calculations in this paper were made using the System for Atmospheric Model-
4 ing (SAM; Khairoutdinov and Randall 2003). Two model runs were performed, configured
5 as standard Global Energy and Water Cycle Experiment (GEWEX) Cloud System Studies
6 (GCSS; Randall et al. 2003) experiments: a Barbados Oceanographic and Meteorological
7 Experiment (BOMEX; Siebesma et al. 2003) run, and an Atmospheric Radiation Measure-
8 ment Study (ARM; Brown et al. 2002) run. The BOMEX run was performed on a 6.4 km
9 x 6.4 km horizontal x 3.2 km vertical domain with 25 meter grid size in all directions for 6
10 hours, and the first three hours of simulation were discarded. The ARM run was performed
11 on a 7.68 km x 7.68 km x 4.5 km domain with 30 meter grid size. Precipitation was disabled
12 in both runs.

We have implemented the entrainment calculation scheme of Roms (2010) in SAM, allowing us to calculate the mass of air entrained into and detrained from cloud core directly from model ρ , \mathbf{u} , and \mathcal{A} . Roms (2010, eq. 4) also presents a method for calculating local entrainment and detrainment rates for any model variable in the same framework as (4), but neglects forcing and diffusion terms. These terms are significant for quantities like vertical momentum, so we modify Roms' equation to include their effects:

$$e\phi - d\phi = \frac{\partial}{\partial t}(\phi\mathcal{A}\rho) + \nabla \cdot (\phi\rho\mathbf{u}\mathcal{A}) - \rho\mathcal{A}S_\phi. \quad (5)$$

13 where S_ϕ is any non-advective source or sink term for ϕ , such as precipitation for q_t or

1 pressure gradient for w , in units of $[\phi] \text{ s}^{-1}$. The inclusion of these source/sink terms allows
 2 us to expand the definition of ϕ to include non-conserved fluid properties.

3 As with equation (4), the local $(e\phi)(x, y, z)$ and $(d\phi)(x, y, z)$ must be horizontally summed
 4 to give the total entrainment into or detrainment out of the cloud ensemble for any fluid
 5 property, but since ϕ can be negative for properties like vertical velocity, it is possible for
 6 entrainment to reduce and for detrainment to increase the various properties of the cloud
 7 core. To accommodate this effect, if the average value of ϕ is positive over the time that a grid
 8 cell experiences mass fluxes between an active and an inactive grid cell, then positive $e\phi - d\phi$
 9 values are considered to be purely $e\phi$, and negative values, $d\phi$. However, if the average of
 10 ϕ is negative, then positive $e\phi - d\phi$ values are considered to be purely $(d\phi)(x, y, z)$, and
 11 negative values, $(e\phi)(x, y, z)$.

12 The obvious way to calculate the average value of ϕ is to perform a flux-weighted cal-
 13 culation, so that $\phi = (e\phi - d\phi)/(e - d)$. However, doing so for positive definite quantities,
 14 such as q_t , sometimes results in negative ϕ . The see the reason for this, consider a situation
 15 where $(e - d)$ integrated over the period of activity is found to be slightly bigger than zero
 16 for a grid cell. The Romps algorithm would assign E to a small value and D to be zero,
 17 but in reality the problem is unconstrained; as long as $E \approx D$, the net flux measured by the
 18 algorithm would be satisfied. At the same time, $Eq_t - Dq_t$ is found to be negative, due to
 19 E and D having similar magnitudes but the detraining q_t being larger than the entraining q_t .
 20 In this case, $(Eq_t - Dq_t)/(E - D)$ will be negative, even though q_t is always positive. To
 21 avoid this problem, we calculate ϕ as a simple time average for the purpose of determining
 22 if $e\phi - d\phi$ is assigned to $e\phi$ or to $d\phi$. Horizontal summation of $(e\phi)$ and $(d\phi)$ then gives
 23 $(E\phi)_d(z)$ and $(D\phi)_d(z)$, the total entrainment and detrainment of a property for the cloud

ensemble in units of $[\phi] \text{ kg s}^{-1} \text{ m}^{-3}$ calculated directly from the model velocity and property fields.

3. Relationship Between Direct and Tracer Budget Entrainment

Romps (2010) established that the direct estimate of mass entrainment and detrainment yields values roughly twice the size of those calculated via conserved tracer budgets. Furthermore, examination of the ratios of the Siebesma mass entrainment and detrainment calculated via a total specific water budget (E_{qS} , D_{qS}) to the directly calculated values (E_d , D_d) over the diurnal cycle of an ARM LES reveals significant changes over the course of the day (Fig. 1). Thus, the tracer and direct measurements of E and D are not only significantly different, but have differing dynamics, which may need to be accounted for in large-scale parametrizations that account for entrainment and detrainment. In this section we examine the sources of disagreement between direct and Siebesma tracer budget estimates of mass entrainment into and detrainment from the cloud core. We first consider the different assumptions about tracer values in the cloud core and environment, then look at relationships between entrainment/detrainment and tracer values and the different numerical approximations made in the Siebesma tracer budget and direct calculations.

1 *a. E and D Cloud Shell Correction*

2 Romps attributed the differences between $(E_{\phi S}, D_{\phi S})$ and (E_d, D_d) to the assumption
3 made by Siebesma and Cuijpers (1995) that fluid entrained or detrained has the properties
4 of the mean environment or cloud core, respectively. The fact that the mean core and
5 environment properties are not representative of entraining and detraining fluid is shown in
6 Fig. 2a. If we examine the horizontal mean specific humidity of the fluid at the “cloud core
7 edge” (cloud core model grid cells that are nearest-neighbor adjacent to non-core cells), which
8 presumably is the fluid being detrained, we see it is drier than the mean core. Similarly, the
9 fluid just outside the cloud core in the “cloud core shell” (non-core model grid cells that are
10 nearest-neighbor adjacent to core cells) which is available for entrainment is moister than
11 the mean environment.

Budget equations that explicitly distinguish between the the moist cloud shell and dry
cloud edge allow us to transform (E_d, D_d) values into equivalent Siebesma tracer budget
values $(E_{\phi S}, D_{\phi S})$ and back again. We start our derivation with the observation that both
the tracer budget and direct value of E and D are consistent with the continuity equation
(equations 2 and 4). This implies that

$$E_{\phi} - D_{\phi} = E_d - D_d. \quad (6)$$

Similarly, the entrainment and detrainment rates of water must be consistent with the total
water budget, giving us

$$E_{\phi}\phi_{env} - D_{\phi}\phi_{core} = E_d\phi_E - D_d\phi_D. \quad (7)$$

Combining these equations and solving for E_ϕ and D_ϕ in turn results in:

$$E_{\phi T} = E_d - \left[E_d \frac{(\phi_E - \phi_{env})}{(\phi_{core} - \phi_{env})} + D_d \frac{(\phi_{core} - \phi_D)}{(\phi_{core} - \phi_{env})} \right] \quad (8a)$$

$$D_{\phi T} = D_d - \left[E_d \frac{(\phi_E - \phi_{env})}{(\phi_{core} - \phi_{env})} + D_d \frac{(\phi_{core} - \phi_D)}{(\phi_{core} - \phi_{env})} \right]. \quad (8b)$$

Here we have added the T subscript to the $E_{\phi T}$ and $D_{\phi T}$ terms to denote that these values are equivalent to Siebesma tracer budget values, but have been calculated by transforming the direct entrainment and detrainment values. We shall refer to these values as “transformed” entrainment and detrainment. The bracketed terms represent the bias introduced by assuming that entrained/detrained air has the properties of the mean environment and core. Thus, to convert from (E_d, D_d) to $(E_{\phi T}, D_{\phi T})$, both E_d and D_d must be reduced by $E_d A + D_d B$, where $A = (\phi_E - \phi_{env})/(\phi_{core} - \phi_{env})$ and $B = (\phi_{core} - \phi_D)/(\phi_{core} - \phi_{env})$.

Note that rearrangement of A gives $\phi_E = A\phi_{core} + (1 - A)\phi_{env}$ so A can be thought of as the fraction of mean core air in a mixture of mean core and mean environment air needed to produce the properties of the entrained fluid. Similarly, $\phi_D = B\phi_{env} + (1 - B)\phi_{core}$ and B can be thought of as the fraction of mean environment air in a mixture of mean core and mean environment air needed to produce the properties of the detrained fluid. Since the fluid being entrained or detrained does not necessarily originate at the level it is entrained or detrained at, we cannot assume that a fraction A of the entrained air is modified core air. Nevertheless, A and B are likely proxies for the recirculation of entrained and detrained air.

Alternatively, we can solve for E_d and D_d , arriving at

$$E_{dT} = E_{\phi S} + \left[E_{\phi S} \frac{(\phi_E - \phi_{env})}{(\phi_D - \phi_E)} + D_{\phi S} \frac{(\phi_{core} - \phi_D)}{(\phi_D - \phi_E)} \right]. \quad (9a)$$

$$D_{dT} = D_{\phi S} + \left[E_{\phi S} \frac{(\phi_E - \phi_{env})}{(\phi_D - \phi_E)} + D_{\phi S} \frac{(\phi_{core} - \phi_D)}{(\phi_D - \phi_E)} \right]. \quad (9b)$$

1 In this case, to convert from $(E_{\phi S}, D_{\phi S})$ to (E_{dT}, D_{dT}) , both $E_{\phi S}$ and $D_{\phi S}$ must be increased
2 by $E_{\phi S}a + D_{\phi S}b$, where $a = (\phi_E - \phi_{env})/(\phi_D - \phi_E)$ and $b = (\phi_{core} - \phi_D)/(\phi_D - \phi_E)$. Note
3 that under both these transformations $E_d - D_d = E_\phi - D_\phi$, preserving mass continuity, and
4 furthermore, $E_dA + D_dB = E_\phi a + D_\phi b$.

5 We now have relationships allowing us to transform the unbiased E_d and D_d values into
6 biased Siebesma tracer budget $E_{\phi S}$ and $D_{\phi S}$ values, which are better suited for simple en-
7 training plume parametrization of cloud fields. Comparison of E_{qS} and D_{qS} ($E_{\phi S}$ and $D_{\phi S}$
8 inferred using total specific moisture q_t as the tracer) with E_d and D_d shows the direct
9 entrainment and detrainment magnitudes are significantly larger than the Siebesma tracer
10 budget values (Figure 2b and 2c, grey and dotted lines). Using (8) to calculate E_{qT} and
11 D_{qT} with $q_E = q_{edge}$, the horizontal mean humidity in the cloud edge, and $q_D = q_{shell}$, the
12 horizontal mean humidity in the cloud shell, results in values quite close to the Siebesma
13 tracer budget values above the middle of the cloud layer. The transformation also dupli-
14 cates the negative detrainment values near cloud base that are typically produced by tracer
15 calculations.

16 *b. Preferential Entrainment of Moist, Ascending Air*

17 Relative to the Siebesma tracer budget values, the transformed E_{qT} and D_{qT} values
18 calculated using $q_E = q_{edge}$ and $q_D = q_{shell}$ are still too large near cloud base. We can partially
19 explain the difference between the transformed mass entrainment/detrainment values and the
20 Siebesma tracer budget values as being the result of the mean tracer values of the entrained
21 and detrained air being different than the mean value of the shell and edge air, respectively.

Using the mean shell and edge values of tracers to transform the direct entrainment and detrainment assumes that any fluid parcel in the shell or edge is equally likely to be entrained or detrained. In reality, mixing relatively dry air into the cloud core is more likely to cause evaporation, which will drive detrainment, while mixing relatively moist air into the cloud core is more likely to produce a saturated fluid mixture, resulting in entrainment. This suggests that the moistest shell parcels are more likely to undergo entrainment than the average shell parcel, and the driest edge parcels are more likely to detrain than the average edge parcel.

We can directly calculate the effective tracer value at which entrainment occurs by taking the total tracer entrainment $(E\phi)_d$ calculated via equation (5) and dividing it by the total mass entrainment E_d so that $\phi_{entrain} = (E\phi)_d/E_d$. Similarly, the effective tracer value at which detrainment occurs can be found from $\phi_{detrain} = (D\phi)_d/D_d$. Examination of these values from the BOMEX simulation using q_t for ϕ shows $q_{entrain}$ is moister than q_{shell} (Figure 3a), indicating entrainment occurs preferentially at the moistest parts of the shell. Conversely, there is little difference between $q_{detrain}$ and q_{edge} , indicating the detrained parcels tend to have the mean moisture of the cloud core edge.

Using $q_{entrain}$ and $q_{detrain}$ to transform E_d and D_d results in smaller E_{qT} and D_{qT} values than utilizing the mean shell and edge properties (solid black line, Fig. 3b and 3c). E_{qT} calculated using $q_E = q_{entrain}$ and $q_D = q_{detrain}$ is about half the magnitude of the Siebesma tracer budget entrainment value throughout the cloud layer. This new transformation reduces the large entrainment and detrainment values near cloud base, which improves the overall shape of the fluxes. Above mid-cloud, however, there is less correspondence between transformed E_{qT} and D_{qT} values and the Siebesma tracer budget values E_{qS} and D_{qS} when

1 compared to the shell and edge correction of Figure 3.

2 *c. Tracer Budget Errors*

3 The results above highlight the role of the definition of mean cloud and environmental
4 quantities in determining entrainment and detrainment using tracer budgets. An additional
5 source for the discrepancy between the tracer budgets and their direct counterparts is the cal-
6 culation of source and sink terms. The Siebesma tracer budget calculated using (3) accounts
7 for the vertical advection of tracer properties by taking derivatives of mean vertical tracer
8 profiles, along with averaged vertical Reynolds fluxes. There is no guarantee this estimate
9 of vertical advection will exactly agree with the fully three dimensional MPDATA advection
10 algorithm used by SAM. In fact, the differences in the numerics of these calculations likely
11 insures the results, while similar, will not be exactly the same. Furthermore, the Siebesma
12 calculation neglects tracer diffusion. These effects are likely small, but the exact amount of
13 error they induce is difficult to evaluate.

Romps (2010) presents an alternative to the Siebesma method of calculating tracer budget
entrainment and detrainment values (Romps’ equations (11) and (12)) which uses the direct
mass and ϕ entrainment/detrainment rates and mean profiles of ϕ_{core} and ϕ_{env} to calculate
the vertical advection and time tendency budgets (referred to as VATT below) that are on
the right hand side of (3):

$$E_{\phi R}(\phi_{core} - \phi_{env}) = \phi_{core}(E_d - D_d) - ((E\phi)_d - (D\phi)_d) \quad (10a)$$

$$D_{\phi R}(\phi_{core} - \phi_{env}) = \phi_{env}(E_d - D_d) - ((E\phi)_d - (D\phi)_d) \quad (10b)$$

1 Here the R subscript indicates that E and D have been calculated via the Romps tracer
 2 budget method, and we shall refer to values calculated by this method as the “Romps tracer
 3 budget” E and D .

To see that the Romps tracer budget equations (10) account for exactly the same source
 and sink terms as the Siebesma tracer budget equations (3), first multiply (2) by ϕ_{core} :

$$\phi_{core}(E_d - D_d) = \phi_{core} \left(\rho \frac{\partial a}{\partial t} + \frac{\partial M_{core}}{\partial z} \right). \quad (11)$$

If diffusion is neglected, the tracer continuity equation can be used to show that

$$(E\phi)_d - (D\phi)_d = \rho \frac{\partial(a\phi_{core})}{\partial t} + \frac{\partial(M_{core}\phi_{core})}{\partial z} + \frac{\partial \rho a \overline{w' \phi'}^{core}}{\partial z} - a \rho \left(\frac{\partial \bar{\phi}}{\partial t} \right)_{forcing}. \quad (12)$$

4 Subtracting $(E\phi)_d - (D\phi)_d$ from $\phi_{core}(E_d - D_d)$ then results in the VATT budget terms on
 5 the rhs of (3a).

6 Note that by substituting $(E\phi)_d = E_d\phi_E$ and $(D\phi)_d = D_d\phi_D$ into (10), we can quickly
 7 recover the equations to transform direct entrainment/detrainment values into equivalent
 8 tracer budget values (equations (8a) and (8b)). This equivalence between (8) and (10)
 9 means the Romps tracer budget formulation agrees exactly with the result of using $q_{entrain}$
 10 and $q_{detrain}$ values to transform the direct entrainment and detrainment into equivalent tracer
 11 budget values.

12 Comparing the Romps and Siebesma $q_{core}(E_d - D_d)$ values (Fig. 4a) shows that the Romps
 13 value for this first VATT term has a significantly smaller magnitude than the Siebesma value
 14 given by (3). The Romps $(Eq_t)_d - (Dq_t)_d$ values (Fig. 4b) also have smaller magnitudes
 15 when compared to the Siebesma values. The reason for this can be seen by comparing these
 16 calculations with a version of the direct entrainment calculation done without any time
 17 averaging of the fluxes. The effect of time averaging is to significantly reduce the size of the

1 direct entrainment and detrainment rates E_d and D_d . The difference $E_d - D_d$, however, is
 2 the same with or without time averaging in order to satisfy mass continuity as expressed
 3 by (2). Indeed, the unaveraged $\phi_{core}(E_d - D_d)$ value (gray line in Figure 4a) agrees almost
 4 exactly with the Siebesma tracer budget value $\phi_{core}(E_{qS} - D_{qS})$ (dotted line). Due to the
 5 time averaging of the direct entrainment and detrainment, the direct calculation always has
 6 a pool of “activity flux” which has not yet been assigned to either E_d or D_d . This reduces
 7 both E_d and D_d by roughly the same proportion, causing $E_d - D_d$ to be smaller than both
 8 the unaveraged direct values and the Siebesma $E_{qS} - D_{qS}$ values.

9 However, despite the large differences between the time averaged $q_{core}(E_d - D_d)$ and
 10 $((Eq_t)_d - (Dq_t)_d)$ values and the unaveraged values, the net tracer budget that results from the
 11 difference between these terms (Fig. 4c) agrees remarkably well between the time-averaged
 12 and instantaneous calculations. Conversely, the Siebesma tracer budget that results is much
 13 larger than the Romps tracer budget, despite the close agreement between the Siebesma and
 14 Romps tracer budget $q_{core}(E_d - D_d)$ and $((Eq_t)_d - (Dq_t)_d)$ values. This difference between the
 15 tracer budgets calculated by the Siebesma and Romps methods is the source of the remaining
 16 differences between the direct and Siebesma entrainment and detrainment calculations.

17 Evaluating whether the VATT budget calculation done using (3) or (10) is more accurate
 18 is difficult. We have mentioned the possible problems in the Siebesma tracer budget calcu-
 19 lation related to neglect of tracer diffusion and the simplified method used for calculating
 20 vertical advection. The Romps tracer budget, on the other hand, requires taking the differ-
 21 ence of $q_{core}(E_d - D_d)$ and $((Eq_t)_d - (Dq_t)_d)$, terms which have nearly the same magnitude.
 22 Because the magnitude of these terms is so similar, small relative errors in these terms can
 23 result in large relative errors when their difference is taken. Consider, for example, the tiny

1 difference between the unaveraged direct $((Eq_t)_d - (Dq_t)_d)$ and the Siebesma $((Eq_t)_d - (Dq_t)_d)$
2 calculated via (12) (Fig. 4b). Although the Siebesma tracer budget $((Eq_t)_d - (Dq_t)_d)$ differs
3 only slightly from the unaveraged direct flux value, this results in a relatively large difference
4 between the unaveraged direct tracer budget and Siebesma tracer budgets (Fig. 4c). Both
5 of the calculation methods thus have possible sources of error.

6 4. E_q , E_h and E_w Differences

7 Equations (8a) or (8b) imply that the Siebesma tracer budget method will measure
8 different entrainment and detrainment values for fluid properties with differing values of
9 $A = (\phi_E - \phi_{env})/(\phi_{core} - \phi_{env})$ and $B = (\phi_{core} - \phi_D)/(\phi_{core} - \phi_{env})$. With this in mind we
10 compare transformed $E_{\phi T}$ and $D_{\phi T}$ values produced by liquid water moist static energy h
11 and vertical velocity w with those produced using total specific moisture q_t .

12 Liquid water moist static energy shows a similar relative distribution of core, edge, shell,
13 environment, entrained, and detrained properties when compared to q_t , indicating a tight
14 coupling between these variables in the cloud dynamics. Because these properties are so
15 tightly coupled, the transformed E_{hT} and D_{hT} values are nearly identical to the E_{qT} and
16 D_{qT} (not shown).

17 Vertical velocity shows very different relative profiles compared to q_t or h (c.f. Fig. 5a
18 and Fig. 3a). There is a much wider spread in the w values, with the shell having nearly zero
19 vertical velocity and the edge being halfway between the core and the environment. $w_{detrain}$
20 is slightly larger than the value of w in the cloud core edge, while $w_{entrain}$ is much larger than
21 w in the shell, becoming roughly the same value as w_{edge} . Since $w_{entrain}$ and $w_{detrain}$ are both

larger than w_{shell} and w_{edge} this implies that rapidly rising air is both preferentially entrained and detrained over slowly rising air. These effective entrainment and detrainment w values produce E_{wT} and D_{wT} (solid black line, Fig. 5c and Fig. 5c) that are quite different than the transformed entrainment and detrainment produced by q_t and h (dotted line, Fig. 5b and 5c); E_{wT} is negative over the whole of the cloud field, and D_{wT} is half the magnitude of D_{qT} over much of the cloud layer.

Finally, we examine the temporal variability of $A = (\phi_E - \phi_{env})/(\phi_{core} - \phi_{env})$ and $B = (\phi_{core} - \phi_D)/(\phi_{core} - \phi_{env})$ from the transformation equations (8a) and (8b) in the ARM model run. Since A represents the fraction of core air in a mixture of core and environmental air which has the properties of ϕ_E , and B represents the fraction of environmental air in a mixture of core and environmental air which has the properties of ϕ_D , A and B provide information about the amount of recirculation of entrained and detrained fluid occurring at different model heights. However, A and B cannot be considered exact mixing fractions, as the source heights of air mixtures may be different than the height at which they entrain or detrain, and not all mixtures of core and environment properties are equally likely to undergo entrainment.

A and B calculated for q_t both show strong changes over the ARM diurnal cycle (Figure 6, a and b). Near cloud base, A is nearly one while B is nearly zero, implying that both the entrained and detrained air have the properties of the cloud core air. This is due to the main entrainment process at cloud base being condensation of rising thermals instead of mixing; buoyant updrafts simply condense without modification of their properties. Similarly, the air that detrains from the clouds at cloud base is almost undiluted because most entrainment at this level comes from the well-mixed sub-cloud layer below and so has properties nearly

1 identical to the cloud core. At cloud top, A is also nearly one while B is nearly zero, implying
 2 that both the entrained and detrained air have the properties of the cloud core air. Here,
 3 this is due to the main detrainment process from the core being clouds becoming negatively
 4 buoyant as θ_v in the inversion increases faster than heating due to condensation can add
 5 buoyancy to the cloud core (Wu et al. 2009). Since this process does not depend on mixing,
 6 the air detraining from the core is relatively undiluted by the environment. Conversely,
 7 much of the air surrounding the remaining cloud core which is available for entrainment was
 8 previously detrained from the core without mixing, and so has the properties of the core air.

9 As the clouds mix into the inversion over the course of the day, they cause the inversion
 10 to rise. This means that points in the mid-cloud layer are less influenced by the adiabatic
 11 entrainment and detrainment processes occurring at cloud base and cloud top, and so the
 12 effects of mixing become more prominent. By the end of the day, A within the cloud layer
 13 has values near 0.6, suggesting that a significant amount of re-entrainment of air previously
 14 detrained from the core still occurs. B has values near 0.2, indicating that air detraining
 15 from the core is relatively undiluted by environmental air; this is sensible, since relatively
 16 little dilution by environmental air is required to cause the core air to become neutrally
 17 buoyant and detrain.

18 When calculated for w on the other hand, A reaches a value around 0.4 and B goes to
 19 0.6. The difference between these values and the values of A and B calculated for q_t is the
 20 result of buoyancy and pressure gradient forces on the mixtures, and the stronger tendency
 21 for upward-moving shell parcels to be entrained relative to the tendency to entrain moister
 22 shell parcels. In other words, a relatively dry, rapidly ascending shell parcel is more likely
 23 to be entrained than a relatively moist, slowly ascending shell parcel. This is especially

1 apparent near cloud base where the values of A are larger than 1, due to the mean entrained
2 parcels having a larger upward velocity than the mean core parcels.

3 Performing these calculations with fixed values of $(\phi_{core} - \phi_{env})$, to remove changes due
4 to movement of the mean environment and core profiles, shows similar results. Changes
5 in the properties of the entraining and detraining fluid due to the dynamics of mixing and
6 entrainment in the shell clearly are active in determining the rates at which properties entrain
7 and detrain.

8 **5. Causes of Preferential Entrainment of Moist, As-** 9 **cending Air**

10 The reason that shell air which is moister and ascending faster than the mean shell is more
11 likely to be entrained can be seen by comparing instantaneous snapshots of the model values
12 of local mass entrainment e , moisture entrainment eq_t , and vertical velocity entrainment ew .
13 Since the Romps (2010) method of calculating e and d requires taking time averages, it is
14 unsuitable for calculating instantaneous entrainment fields. Instead, we use an alternative
15 method we have devised that substitutes spatial interpolation for time averaging (Dawe and
16 Austin 2011). This alternative method results in slightly smaller values of e and d than those
17 produced by Romps' method, but the two calculations show good agreement in variability.
18 The eq_t and ew fields are calculated simply by multiplying the value of e by the values of q_t
19 and w , respectively.

20 Comparing the e , eq_t , and ew fields shows that e and eq_t have a very similar spatial

1 pattern, but ew is concentrated in regions where strong updrafts enter the cloud core (Figure
 2 7). The reason for this can be seen by examining the buoyancy, condensed liquid water,
 3 and vertical velocity fields that define the cloud core. Of these three fields, buoyancy is the
 4 strongest constraint determining if air is part of the core. However, regions exist far above
 5 cloud base where air has become negatively buoyant but maintains upward velocity and
 6 condensed liquid water. As this air continues to rise more condensation occurs, which heats
 7 the updraft, makes it positively buoyant, and thus entrains it into the core. In this way,
 8 entrainment is positively correlated with both q_t and w . This process occurs fairly often in
 9 our model cloud field, as evidenced both by our manual examination of the output fields,
 10 and the size of the difference between w_{shell} and $w_{entrain}$ in the mean profiles.

11 6. Discussion

12 Considering all these results, we now turn to the most important question of all: which
 13 entrainment value is the right one? The unsatisfying answer is that it depends on the purpose
 14 for which the entrainment is to be used.

Consider a cumulus cloud parametrization based upon a simplified form of the continuity
 equation which assumes the cloud fraction is constant,

$$\frac{\partial M_{core}}{\partial z} = E - D \quad (13)$$

a cloud budget equation that assumes mean vertical advection is balanced by entrainment
 of mean environmental properties,

$$M_{core} \frac{\partial \phi_{core}}{\partial z} = E(\phi_{env} - \phi_{core}) \quad (14)$$

and a simple detrainment forcing equation,

$$\rho \frac{\partial \phi_{env}}{\partial t} = D(\phi_{core} - \phi_{env}). \quad (15)$$

1 ϕ_{env} is input to the parametrization from the GCM. If we assume we have a perfect parametriza-
2 tion of M_{core} and ϕ_{core} at cloud base with which to construct mean core mass flux and tracer
3 profiles, we wish the E and D values to produce a profile of $\partial \phi_{core} / \partial t$ to force the GCM
4 which agrees with LES results for a similar mean environmental profile. The E and D we
5 desire then is closer to E_{ϕ_S} and D_{ϕ_S} than E_d and D_d , but nevertheless must be modified
6 to account for the time tendency and Reynolds flux budget terms we have neglected. This
7 also implies that we should have different E_{ϕ_S} and D_{ϕ_S} values for properties with different
8 distribution patterns around the clouds.

Using values near E_d and D_d instead would require modifying equation (14) to

$$M_{core} \frac{\partial \phi_{core}}{\partial z} = E(\phi_{core} - \phi_E) - D(\phi_{core} - \phi_D) \quad (16)$$

and equation (15) into

$$\rho \frac{\partial \phi_{env}}{\partial t} = D(\phi_D - \phi_{env}) - E(\phi_E - \phi_{env}). \quad (17)$$

9 Now, instead of calculating different E and D values for each tracer we wish to model, we
10 must instead calculate ϕ_E and ϕ_D values for each property that is entrained or detrained.
11 While it is possible this would produce a better parametrization, it seems simpler to fold the
12 effects of ϕ_E and ϕ_D into the E and D values and keep the equations in their less complex
13 form.

14 On the other hand, the true values of the mass entrainment and detrainment are impor-
15 tant for comparison of LES results with field studies, or possibly for calculations of aerosol

1 reactions whose chemical properties are dependent on the concentration of liquid water in
2 the air (Hoppel et al. 1994). They are also vital for diagnosing mass exchanges of individual
3 clouds in an LES ensemble, for which a simple “environment” and “cloud core” mean tracer
4 budget may be difficult to define.

5 The large positive value of $w_{entrain}$ is clearly inconsistent with the often-made assump-
6 tion that fluid entrained into the cloud core has negligible vertical momentum (Simpson and
7 Wiggert 1969; Gregory 2001; Siebesma et al. 2003). This is reflected in the negative magni-
8 tude for the transformed E_{wT} shown in Fig. 5b and the smaller value of D_{wT} compared with
9 D_{qT} in Fig. 5c: since w_{env} is slightly negative, the transformed velocity entrainment must
10 be negative to bring positive velocity into the core. The negative w entrainment values (and
11 the large negative detrainment values produced near cloud base for both q_t and w) empha-
12 size the artificial nature of the Siebesma tracer budget entrainment and detrainment. The
13 Siebesma entrainment and detrainment values are mathematical quantities that satisfy both
14 the continuity equation (2) and the tracer budget of the cloud core under the assumption
15 that the core entrains mean environment fluid and detrains mean cloud core fluid.

16 While the tendency for rapidly ascending shell air to be entrained more often than the
17 slower parts of the shell was found for cloud core entrainment, we would like to emphasize
18 that this process is not an artifact of the cloud core sampling; similar results appear when we
19 perform entrainment calculations for simple cloudy regions (areas of condensed liquid water).
20 In this case, vertical advection of air can drive condensation, converting environment air into
21 cloud air, and thus driving entrainment of air into the cloud.

22 As both BOMEX and ARM model runs involved non-precipitating shallow cumulus, we
23 have ignored the effects of precipitation. Precipitation is generally not considered part of the

1 turbulent mixing processes associated with entrainment and detrainment in parametrization,
 2 instead being represented by a sink term in the liquid water budget (Tiedtke 1989; Kain and
 3 Fritsch 1990). Nevertheless, incorporating precipitation into the Siebesma tracer budget and
 4 direct entrainment calculations would be relatively simple. The precipitation flux divergence
 5 rate would be a new sink/source forcing term in Siebesma’s equation (3), and would be part
 6 of the forcing term ρAS_ϕ in Romps’ equation (5), resulting in precipitation flux divergence
 7 not being counted as part of the detrainment. Specifying the advection terms would be
 8 somewhat trickier since, depending on the complexity of the microphysics scheme, moisture
 9 might be advected as a single q_t field or advected as separate hydrometeor classes. However,
 10 this would simply mean adding extra advection terms for each hydrometeor class. Once
 11 these effects were properly incorporated into the calculations, the transformations between
 12 (E_d, D_d) and (E_{qT}, D_{qT}) would be unchanged.

13 **7. Conclusion**

14 We have explained the differences between values of entrainment and detrainment of
 15 mass calculated via tracer budgets and direct flux calculations by taking into account the
 16 properties of the cloud shell, the tendency for the mean tracer values of the entrained fluid
 17 to be greater than the mean tracer value of the cloud shell, and differences in the numerical
 18 methods used by the two calculations. Furthermore, the tendency for the moistest, fastest-
 19 rising regions of the shell to be entrained more often than the drier, slower parts appears to
 20 be the result of upward advection of negatively buoyant, saturated air so that condensation
 21 causes latent heating, making the air buoyant and entraining it into the core. These effects

1 suggest that the dynamics of the moist cloud shell have a significant role in mediating fluxes
2 between the clouds and the environment.

3 Direct entrainment and detrainment calculations should be used to help improve our
4 understanding of the dynamics of cloud mass exchanges and radial variation in cloud prop-
5 erties, with an eye to folding these effects into the simplest cloud parametrization possible.
6 This should include using the behavior of various tracers to produce different E and D val-
7 ues for q_t and h than for w , and possibly other cloud properties as well. Doing so has the
8 potential to improve GCM parametrization of the magnitude and variability of mass and
9 tracer exchanges between clouds and their environment.

10 *Acknowledgments.*

11 Support for this work was provided by the Canadian Foundation for Climate and Atmo-
12 spheric Science through the Cloud Aerosol Feedback and Climate network. We thank Marat
13 Khairoutdinov for making SAM available to the cloud modeling community. We would also
14 like to thank David Romps and two anonymous reviewers whose comments significantly im-
15 proved the quality of this paper. All figures were generated using the matplotlib library in
16 the Python programming language.

APPENDIX

1

2

Table of Notation

3

4

Table 1 goes here.

REFERENCES

- 3 Bechtold, P., M. Koehler, T. Jung, F. Doblas-reyes, M. Leutbecher, M. J. Rodwell, F. Vitart,
4 and G. Balsamo, 2008: Advances in simulating atmospheric variability with the ECMWF
5 model: From synoptic to decadal time-scales. *Q. J. R. Meteorol. Soc.*, **134** (**634**, **Part**
6 **A**), 1337–1351, doi:10.1002/qj.289.
- 7 Brown, A. R., et al., 2002: Large-eddy simulation of the diurnal cycle of shallow cumulus
8 convection over land. *Q. J. R. Meteorol. Soc.*, **128**, 1075–1093.
- 9 Dawe, J. T. and P. H. Austin, 2011: Interpolation of LES cloud surfaces for use in direct
10 calculations of entrainment and detrainment, submitted to Monthly Weather Review.
- 11 de Rooy, W. C. and A. P. Siebesma, 2010: Analytical expressions for entrainment and
12 detrainment in cumulus convection. *Q. J. R. Meteorol. Soc.*, **136** (**650**), 1216–1227, doi:
13 10.1002/qj.640.
- 14 Gregory, D., 2001: Estimation of entrainment rate in simple models of convective clouds. *Q.*
15 *J. R. Meteorol. Soc.*, **127** (**571**, **Part A**), 53–72.
- 16 Heus, T. and H. J. J. Jonker, 2008: Subsiding shells around shallow cumulus clouds. *J.*
17 *Atmos. Sci.*, **65**, 1003–1018.
- 18 Heus, T., C. F. J. Pols, H. J. J. Jonker, H. E. A. V. den Akker, and D. H. Lenschow, 2009:
19 Observational validation of the compensating mass flux through the shell around cumulus
20 clouds. *Q. J. R. Meteorol. Soc.*, **135**, 101–112.

- 1 Hoppel, W. A., G. M. Frick, J. Fitzgerald, and R. E. Larson, 1994: Marine boundary-layer
2 measurements of new particle formation and the effects nonprecipitating clouds have on
3 aerosol-size distribution. *J. Geophys. Res.-Atmos.*, **99**, 14 443–14 459.
- 4 Jonas, P. R., 1990: Observations of cumulus cloud entrainment. *Atmos. Res.*, **25**, 105–127.
- 5 Jonker, H. J. J., T. Heus, and P. P. Sullivan, 2008: A refined view of vertical mass transport
6 by cumulus convection. *Geophys. Res. Let.*, **35**, L07 810.
- 7 Kain, J. S. and J. M. Fritsch, 1990: A one-dimensional entraining/detraining plume model
8 and its application in convective parameterization. *J. Atmos. Sci.*, **47**, 2784–2802.
- 9 Khairoutdinov, M. F. and D. A. Randall, 2003: Cloud resolving modeling of the arm summer
10 1997 iop: model formulation, results, uncertainties, and sensitivities. *J. Atmos. Sci.*, **60**,
11 607–625.
- 12 Randall, D., et al., 2003: Confronting models with data: The GEWEX cloud
13 systems study. *Bulletin of the American Meteorological Society*, **84** (4), 455–469,
14 doi:10.1175/BAMS-84-4-455, URL <http://journals.ametsoc.org/doi/abs/10.1175/BAMS-84-4-455>,
15 <http://journals.ametsoc.org/doi/pdf/10.1175/BAMS-84-4-455>.
- 16 Rodts, S. M. A., P. G. Duynkerke, and H. J. J. Jonker, 2003: Size distributions and dynam-
17 ical properties of shallow cumulus clouds from aircraft observations and satellite data. *J.*
18 *Atmos. Sci.*, **60**, 1895–1912.
- 19 Romps, D. M., 2010: A direct measure of entrainment. *J. Atmos. Sci.*, **67** (6), 1908–1927.

- 1 Rougier, J., D. M. H. Sexton, J. M. Murphy, and D. Stainforth, 2009: Analyzing the cli-
- 2 mate sensitivity of the HADSM3 climate model using ensembles from different but related
- 3 experiments. *J. Climate*, **22** (13), 3540–3557, doi:10.1175/2008JCLI2533.1.
- 4 Siebesma, A. P., 1998: Shallow cumulus convection. *Buoyant Convection in Geophysical*
- 5 *Flows*, E. J. Plate, Ed., Kluwer Academic Publishers, 441–486.
- 6 Siebesma, A. P. and J. W. M. Cuijpers, 1995: Evaluation of parametric assumptions for
- 7 shallow cumulus convection. *J. Atmos. Sci.*, **52**, 650–666.
- 8 Siebesma, A. P., et al., 2003: A large eddy simulation intercomparison study of shallow
- 9 cumulus convection. *J. Atmos. Sci.*, **60** (10), 1201–1219.
- 10 Simpson, J. and V. Wiggert, 1969: Models of precipitating cumulus towers. *Mon. Wea. Rev.*,
- 11 **97** (7), 471.
- 12 Stainforth, D. A., et al., 2005: Uncertainty in predictions of the climate response to rising
- 13 levels of greenhouse gases. *Nature*, **433**, 403–406.
- 14 Tiedtke, M., 1989: A comprehensive mass flux scheme for cumulus parameterization in
- 15 large-scale models. *Mon. Wea. Rev.*, **117**, 1779–1800.
- 16 Wang, Y. and B. Geerts, 2010: Humidity variations across the edge of trade wind cumuli:
- 17 Observations and dynamical implications. *Atmos. Res.*, **97** (1-2), 144 – 156, doi:DOI:10.
- 18 1016/j.atmosres.2010.03.017, URL [http://www.sciencedirect.com/science/article/](http://www.sciencedirect.com/science/article/B6V95-4YPPPTH-2/2/7398151adf50038f1b76265010f57c38)
- 19 [B6V95-4YPPPTH-2/2/7398151adf50038f1b76265010f57c38](http://www.sciencedirect.com/science/article/B6V95-4YPPPTH-2/2/7398151adf50038f1b76265010f57c38).

- ¹ Wu, C.-M., B. Stevens, and A. Arakawa, 2009: What controls the transition from shallow
² to deep convection? *J. Atmos. Sci.*, **66**, 1793–1806.

¹ List of Tables

²	1	List of Symbols	31
--------------	---	-----------------	----

TABLE 1. List of Symbols

Symbol	Units	Definition	First Occurrence
E, D	$\text{kg m}^{-3} \text{s}^{-1}$	Cloud core mass entrainment/detrainment rate	(2)
$E_{\phi S}, D_{\phi S}$	$\text{kg m}^{-3} \text{s}^{-1}$	Mass entrainment/detrainment rate calculated using Siebesma tracer budget	(3a), (3b)
e, d	$\text{kg m}^{-3} \text{s}^{-1}$	Local mass entrainment/detrainment rate	(4)
E_d, D_d	$\text{kg m}^{-3} \text{s}^{-1}$	Cloud core mass entrainment/detrainment rate calculated directly from model velocity and tracer fields	§1
$e\phi, d\phi$	$[\phi] \text{kg m}^{-3} \text{s}^{-1}$	Local cloud core ϕ entrainment/detrainment rate	(5)
$(E\phi)_d, (D\phi)_d$	$[\phi] \text{kg m}^{-3} \text{s}^{-1}$	Cloud core ϕ entrainment/detrainment rate calculated directly from model velocity and tracer fields	§2
$E_{\phi T}, D_{\phi T}$	$\text{kg m}^{-3} \text{s}^{-1}$	Cloud core mass entrainment/detrainment rate calculated by transforming a directly calculated value into an equivalent tracer budget value	(8a), (8b)
E_{dT}, D_{dT}	$\text{kg m}^{-3} \text{s}^{-1}$	Cloud core mass entrainment/detrainment rate calculated by transforming a tracer budget value into an equivalent directly calculated value	(9a), (9b)
$E_{\phi R}, D_{\phi R}$	$\text{kg m}^{-3} \text{s}^{-1}$	Cloud core mass entrainment/detrainment rate calculated using Roms tracer budget	(10a), (10b)
ϕ	$[\phi]$	Any fluid tracer, such as q_t (kg kg^{-1}), h (J kg^{-1}), or w (m s^{-1})	§1
ϕ_{core}	$[\phi]$	Mean cloud core ϕ	§3a
ϕ_{edge}	$[\phi]$	Mean cloud edge ϕ	§3a
ϕ_{shell}	$[\phi]$	Mean cloud shell ϕ	§3a
ϕ_{env}	$[\phi]$	Mean environment ϕ	§3a
$\phi_{entrain}$	$[\phi]$	Effective value of ϕ being entrained calculated from direct entrainment	§3b
$\phi_{detrain}$	$[\phi]$	Effective value of ϕ being detrained calculated from direct detrainment	§3b
ϕ_E	$[\phi]$	Placeholder for the value of ϕ assumed to be entraining	(8a)
ϕ_D	$[\phi]$	Placeholder for the value of ϕ assumed to be detraining	(8b)

- 1
- 2
- 3
- 4
- 5
- 6
- 7
- 8
- 9
- 10
- 11
- 12
- 13
- 14
- 15
- 16
- 17
- 18
- 19
- 20
- 21

- 2
- 3
- 4
- 5
- 6
- 7
- 8
- 9
- 10
- 11
- 12
- 13
- 14
- 15
- 16
- 17
- 18
- 19
- 20
- 21

- 1 4 Size of a) $q_{core}(E - D)$, b) $Eq_t - Dq_t$ and c) the resulting cloud core verti-
2 cal advection and time tendency specific humidity budget $VATT = q_{core}(E -$
3 $D) - (Eq_t - Dq_t)$ for the direct entrainment/detrainment (black lines), the
4 direct entrainment/detrainment without time averaging (grey lines), and the
5 Siebesma tracer budget entrainment/detrainment (dotted lines). 38
- 6 5 Result of transforming direct entrainment values into equivalent w budget
7 values. a) Mean profiles of the effective w values being entrained (black line),
8 and detrained (dotted line), overlaid on the mean w values of the core, edge,
9 shell and environment. These w values are used to transform directly calcu-
10 lated values of b) entrainment and c) detrainment (grey line) into equivalent
11 tracer budget values (black line). The entrainment and detrainment values
12 transformed using q_t are shown for comparison (dotted lines). 39
- 13 6 Variation in a) the fraction of core air in a mixture of core and environmenal
14 air needed to produce the mean humidity entrained by the clouds, b) the
15 fraction of environmental air in a mixture of core and environmenal air needed
16 to produce the mean humidity detrained by the clouds, c) the fraction of core
17 air in a mixture of core and environmenal air needed to produce the mean
18 vertical velocity entrained by the clouds, and d) the fraction of environmental
19 air in a mixture of core and environmenal air needed to produce the mean
20 vertical velocity detrained by the clouds, over the duration of the ARM model
21 run. 40

7 Instantaneous vertical cross-section of directly calculated cloud core mass en-
trainment (a), humidity entrainment (b), vertical velocity entrainment (c),
buoyancy (d), condensed liquid water (e), and vertical velocity (f) of a single
model cloud, illustrating the tendency to entrain shell air that is rising faster
than the mean shell. Black lines indicate the edge of the cloud core in each
figure.

41

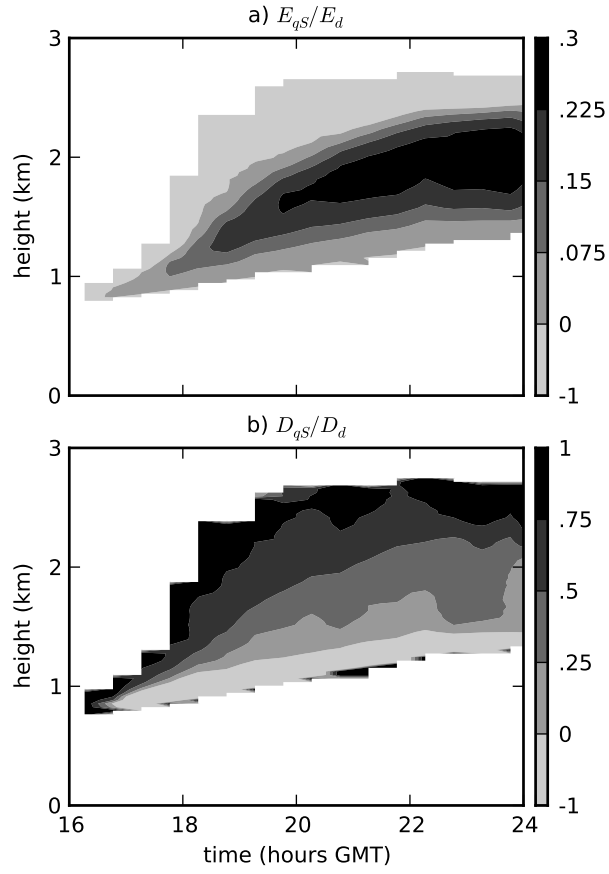


FIG. 1. Ratio of the Siebesma specific humidity tracer budget a) entrainment and b) detrainment values to the directly calculated values over the duration of the ARM model run.

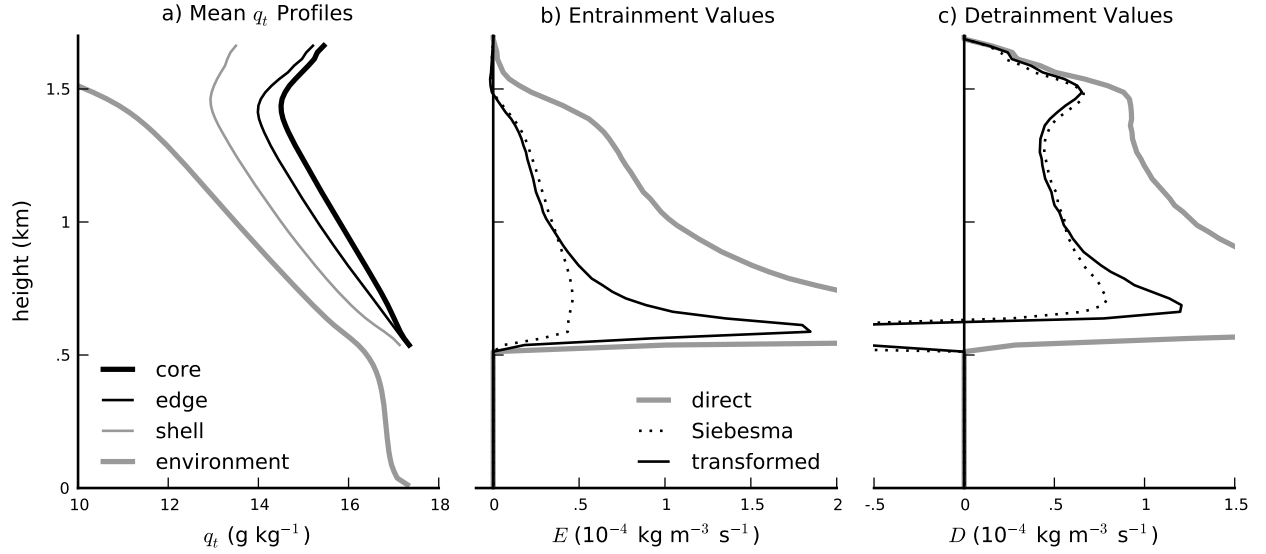


FIG. 2. Result of transforming direct entrainment values into equivalent tracer budget values using mean cloud core shell and edge properties. a) Mean profiles of the total specific humidity in the cloud core (thick black line), cloud core edge (thin black line), cloud core shell (thin grey line), and cloud core environment (thick grey line). These q_t values are used to transform directly calculated values of b) entrainment and c) detrainment (grey line) into equivalent tracer budget values (black line). The Siebesma tracer budget entrainment and detrainment are shown for comparison (dotted lines).

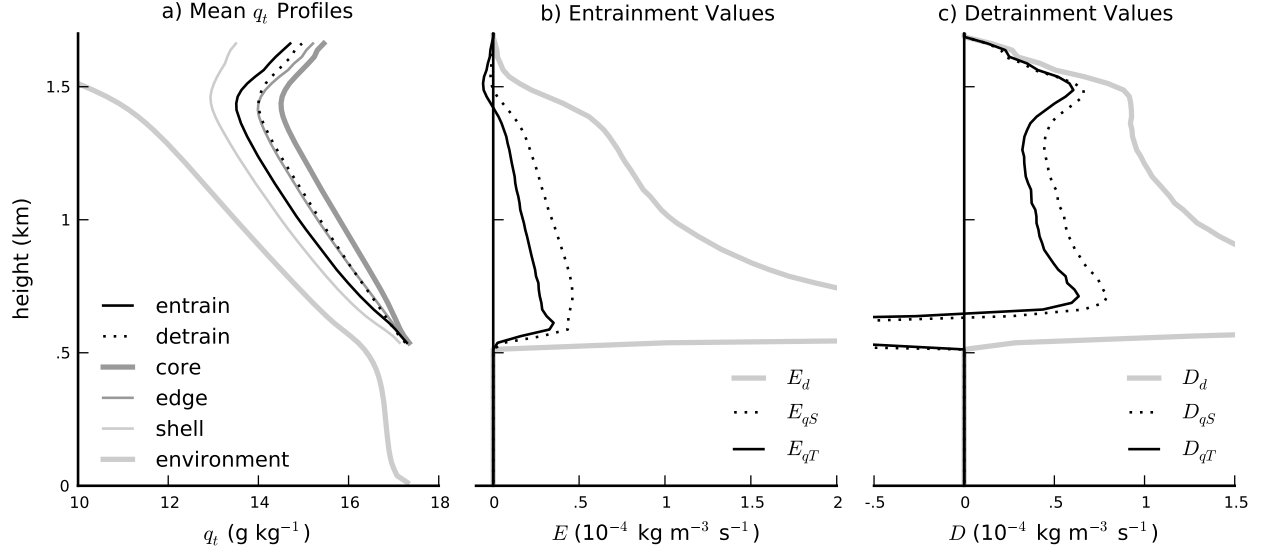


FIG. 3. Result of transforming direct entrainment values into equivalent tracer budget values using effective entrainment and detrainment properties. a) Mean profiles of the effective total specific humidity values being entrained (q_{entrain} , black line), and detrained (q_{detrain} , dotted line), overlaid on the mean total specific humidity values of the core, edge, shell and environment. These q_t values are used to transform directly calculated values of b) entrainment and c) detrainment (grey line) into equivalent tracer budget values (black line). The Siebesma tracer budget entrainment and detrainment are shown for comparison (dotted lines).

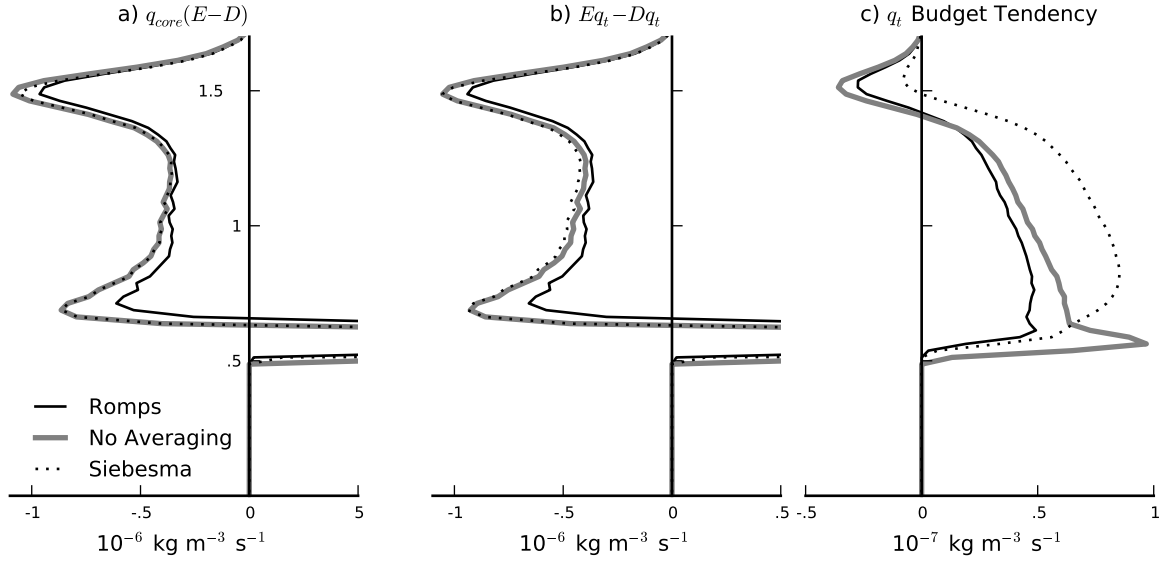


FIG. 4. Size of a) $q_{core}(E-D)$, b) $Eq_t - Dq_t$ and c) the resulting cloud core vertical advection and time tendency specific humidity budget $VATT = q_{core}(E-D) - (Eq_t - Dq_t)$ for the direct entrainment/detrainment (black lines), the direct entrainment/detrainment without time averaging (grey lines), and the Siebesma tracer budget entrainment/detrainment (dotted lines).

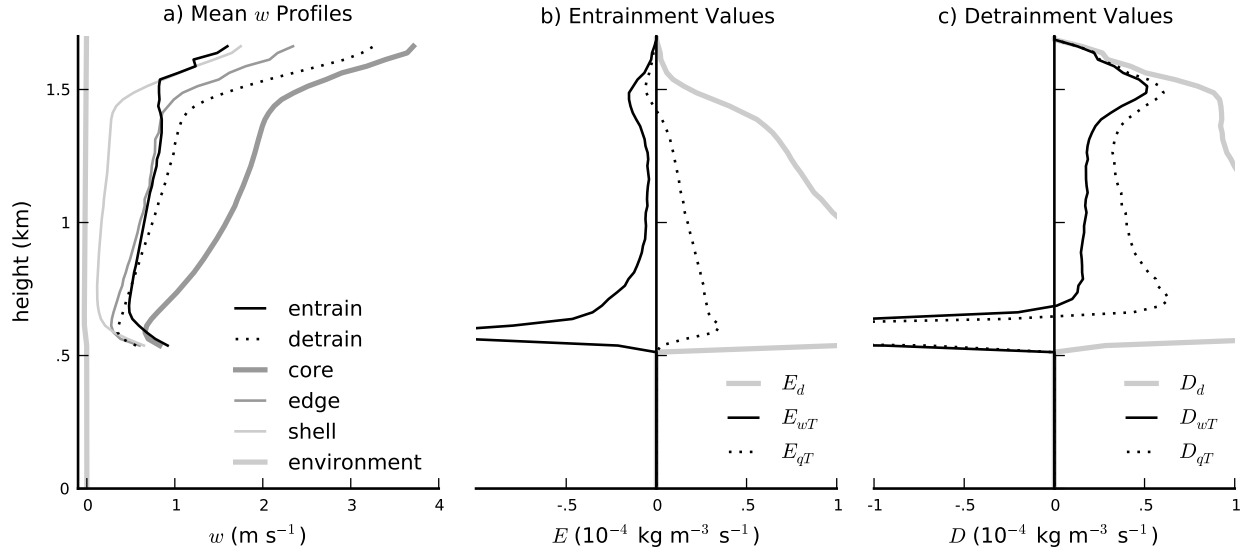


FIG. 5. Result of transforming direct entrainment values into equivalent w budget values. a) Mean profiles of the effective w values being entrained (black line), and detrained (dotted line), overlaid on the mean w values of the core, edge, shell and environment. These w values are used to transform directly calculated values of b) entrainment and c) detrainment (grey line) into equivalent tracer budget values (black line). The entrainment and detrainment values transformed using q_t are shown for comparison (dotted lines).

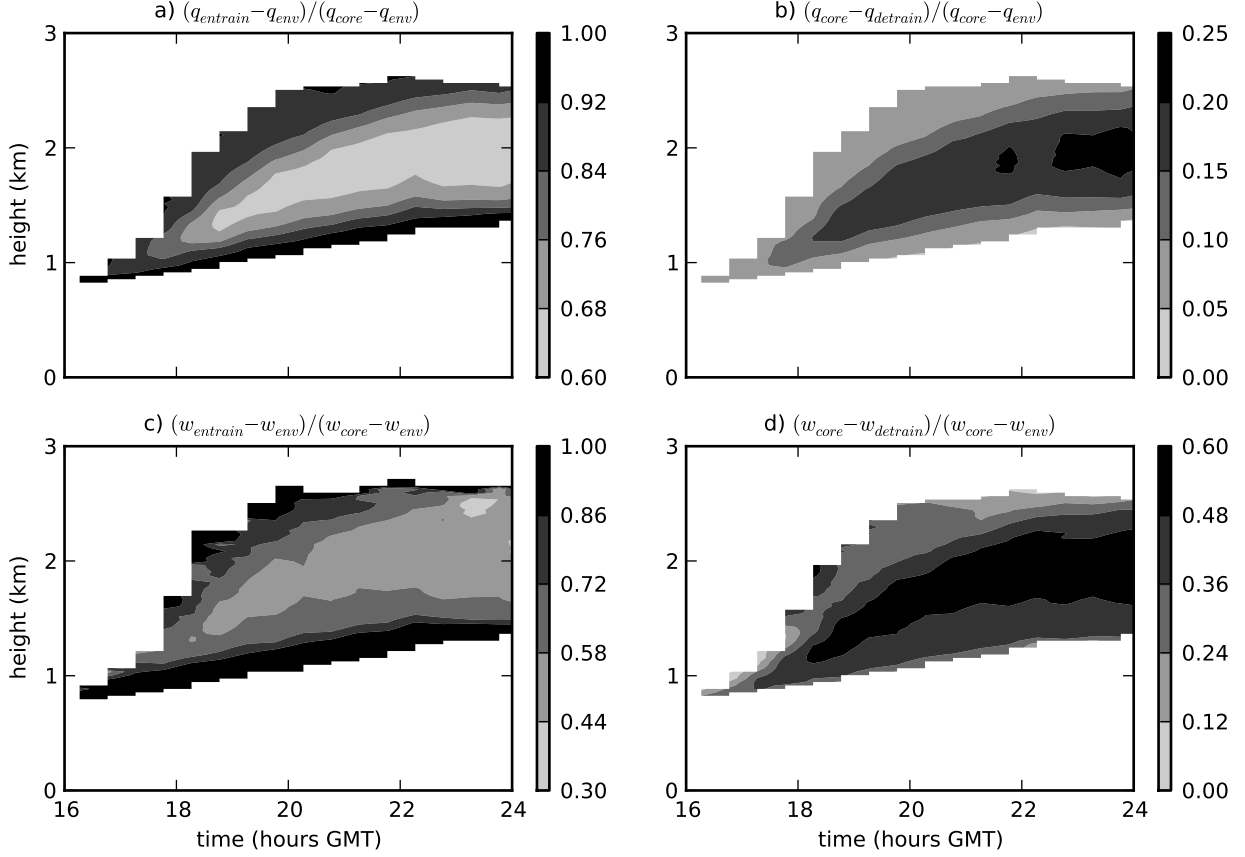


FIG. 6. Variation in a) the fraction of core air in a mixture of core and environmental air needed to produce the mean humidity entrained by the clouds, b) the fraction of environmental air in a mixture of core and environmental air needed to produce the mean humidity detrained by the clouds, c) the fraction of core air in a mixture of core and environmental air needed to produce the mean vertical velocity entrained by the clouds, and d) the fraction of environmental air in a mixture of core and environmental air needed to produce the mean vertical velocity detrained by the clouds, over the duration of the ARM model run.

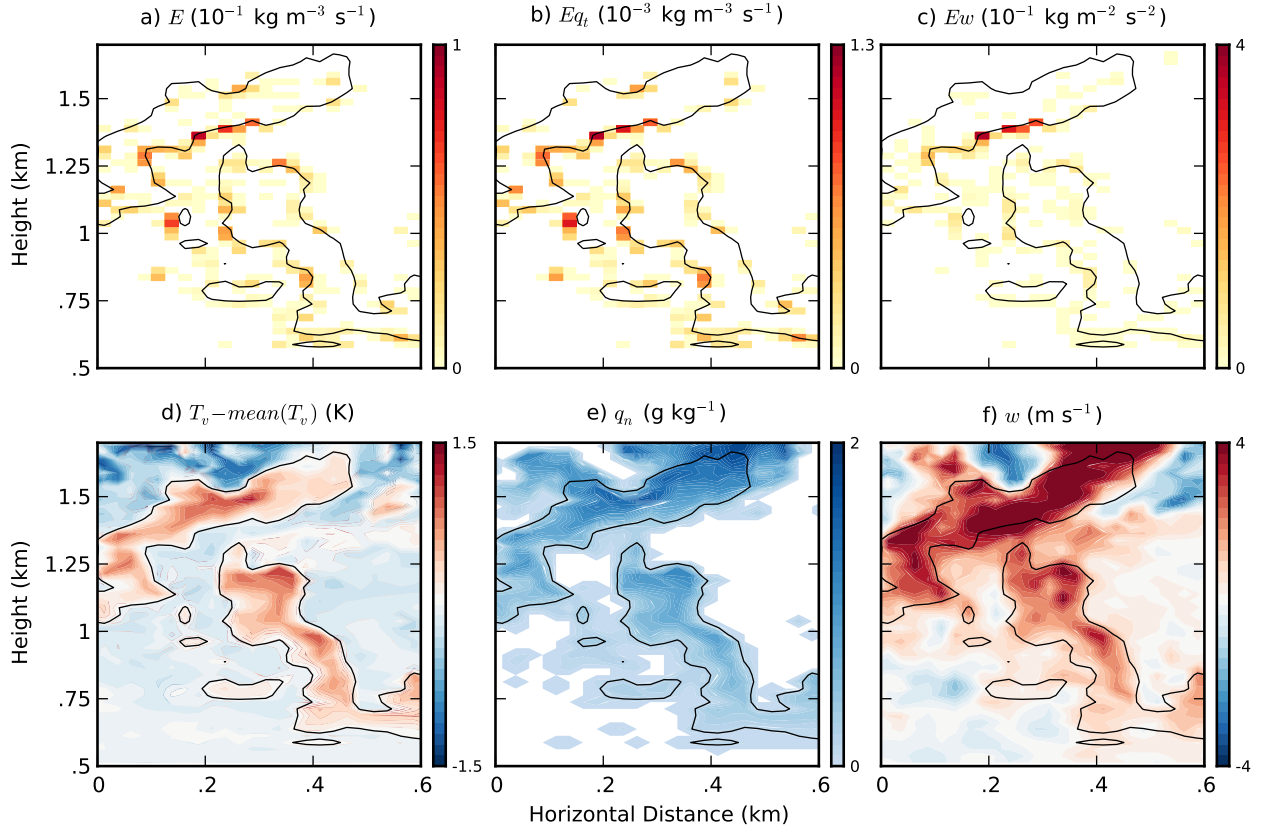


FIG. 7. Instantaneous vertical cross-section of directly calculated cloud core mass entrainment (a), humidity entrainment (b), vertical velocity entrainment (c), buoyancy (d), condensed liquid water (e), and vertical velocity (f) of a single model cloud, illustrating the tendency to entrain shell air that is rising faster than the mean shell. Black lines indicate the edge of the cloud core in each figure.